COLLISIONS & CONTACTS BETWEEN TWO PARTICLES

S. LUDING
Institute for Computer Applications 1
Pfaffenwaldring 27, 70569 Stuttgart, GERMANY
e-mail: lui@ica1.uni-stuttgart.de

Abstract. The alternative to a *continuum model* of granular media (see other chapters in this book) is to view the material as a collection of *discrete particles*. In order to simplify the description, we assume the particles to be spheres in the following. For the characterization of a system with many particles we specify only *two-particle interactions*, assuming many-body interactions to result from the sum of the two-particle forces. The scope of this chapter is to give a summary of frequently used approaches and to compare them.

The applicability of any two-particle interaction model will depend on the properties of the system that are to be described. In static, rather dense, systems frictional interactions are most important, whereas in dynamic, dilute, systems collisional properties dominate. Furthermore, the existence of only binary contacts vs. the possibility of multi-particle contacts influences the response of the system and also the choice of the interaction model.

1. Collisions

First we assume only two particles collide and neglect other particles and external forces like gravity as well.

One possibility for studying a collision is to examine the values of the particles' velocities just before and just after the collision. The collision itself is not necessarily of interest and may be assumed to be instantaneous. These assumptions require the specification of a collision matrix that connects the velocities before with the velocities after the collision, and are used for the event-driven (ED) simulation method [1–3].

Another possibility is to follow the trajectories of the particles also during the collision by solving Newton's equations of motion. Therefore, one

has to specify the forces acting during the contact. As a consequence, the contact takes a finite time, i.e. is *not* instantaneous. The numerical method that uses this collision model will be referred to as molecular dynamics (MD).

In the following, models for two particle interactions will be described. As far as possible, analytical solutions for the movement of the colliding particles will be given and problems connected to the models will be pointed out.

2. The instantaneous collision model

Despite extensive studies of the interaction of two particles [4–11] there exist no conclusive general results. For a detailed theoretical description of two-particle collisions see [12–15] and for a simplified model see [1]. Recent experiments could prove the validity of this simplified model in the range of parameters experimentally accessible [11, 16] and it is used in ED simulations of various systems [1, 3, 17–21].

Given the velocities of the particles just before the contact, three parameters are sufficient to fit the experimental data. These parameters are the restitution coefficient e_n, the coefficient of friction μ and the coefficient of maximum tangential restitution e_{t0}.

2.1. THE RESTITUTION COEFFICIENT e_n

In the normal direction $\hat{\mathbf{n}}$, i.e. parallel to the line connecting the centers of two spherical particles at contact, e_n describes the change in relative momentum (or velocity) in the center of mass reference frame.

$$e_n = -\frac{m_1 v_1'^{(n)} - m_2 v_2'^{(n)}}{m_1 v_1^{(n)} - m_2 v_2^{(n)}} = -\frac{v_1'^{(n)} - v_2'^{(n)}}{v_1^{(n)} - v_2^{(n)}} = -\frac{v_i'^{(n)}}{v_i^{(n)}}. \qquad (1)$$

The particle $i = 1, 2$ has the mass m_i and the velocity $v_i^{(n)}$ and $v_i'^{(n)}$ just before and after the collision respectively. The superscript (n) denotes the component of the velocity parallel to the line connecting the centers of the two particles. The possible values of the restitution coefficient are $0 \leq e_n \leq 1$, where $e_n = 1$ corresponds to an elastic, and $e_n = 0$ to a completely inelastic collision. The total momentum $|m_1\mathbf{v}_1 + m_2\mathbf{v}_2| = |m_1\mathbf{v}_1' + m_2\mathbf{v}_2'| = 0$, is conserved while energy may be lost. As a consequence, Eq. (1) can be verified by using $v_1^{(n)} = -(m_2/m_1)v_2^{(n)}$. Instead of a collision of two particles, the same definition is valid also for the collision of one particle with a flat boundary and infinite mass.

As an example we discuss the case of a ball hitting the horizontal bottom in a gravitational field g. From the initial height h_i and the height of the

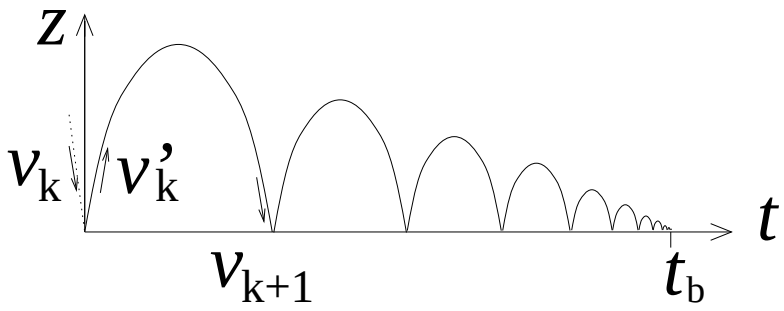

Figure 1. Schematic picture of the height of a jumping particle as a function of time. t_b is the time when the particle has zero velocity.

next bounce h_f, one can calculate the velocity before, $v = \sqrt{2gh_i}$, and after, $v' = -\sqrt{2gh_f}$, the contact. The center of mass is the bottom which is assumed to be immobile. From Eq. (1) we have the restitution coefficient

$$e_n = -\frac{v'}{v} = \sqrt{\frac{h_f}{h_i}}. \tag{2}$$

Note that the restitution coefficient, in general, depends not only on the material but also on the velocity of impact [1, 7, 22–24].

A schematic picture of the particle that carries out several collisions with the bottom is presented in Fig. 1. The velocity after the k-th collision is $v'_k = -e_n v_k$, so that the velocity before the collision $k+1$ is

$$v_{k+1} = e_n v_k = e_n^{k+1} v_0. \tag{3}$$

After 80 collisions, a particle with $e_n = 0.6$ has a velocity of $v_{80} \approx 1.8 \times 10^{-18} v_0$. The time between two successive collisions k and $k+1$ is $t_{k+1} = 2v_{k+1}/g$, and the time t_b until the particle looses all its velocity is the sum over all times between collisions

$$t_b = \sum_{k=0}^{\infty} t_{k+1} = \frac{2v_0 e_n}{g(1-e_n)}. \tag{4}$$

With $v_0 = 6.3$m/s and $e_n = 0.9$ one gets $t_b \approx 11.6$s.

Up to now, each collision was assumed to happen instantaneously. However, an aluminum bead of diameter $d = 1$mm has a typical contact duration of $t_c \approx 1\mu$s [22]. Therefore, the above calculation makes no sense if $t_{k+1} \leq t_c$, i.e. the particle is in steady contact with the bottom after $k_{\max} \approx \log[gt_c/(2v_0)]/\log(e_n)$ collisions.

From this simple example, the limitations of the instantaneous collision model become evident. It can not accurately describe steady, long lasting contacts of particles.

2.2. THE COEFFICIENT OF FRICTION μ

In the tangential direction the coefficient of friction μ determines the active tangential force which is proportional to the normal force but independent of the contact surface. This model is based on experiments by Coulomb [25]. In Fig. 2 the force due to gravity f_N, the friction force f_R, and a pulling force f acting on a block on a flat surface are schematically shown.

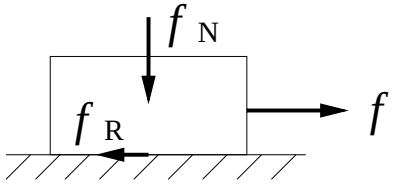

Figure 2. Forces acting on a block on a flat surface.

In general one has to distinguish between static friction with $f_R^s \leq \mu_s f_N$, dynamic friction with $f_R^d = \mu_d f_N$, and rolling friction with $f_R^r \leq \mu_r f_N$. In all of these cases one usually assumes the friction force to be independent of the surface of the contact. Usually one has $\mu_s > \mu_d >> \mu_r$, so that $\mu = \mu_d = \mu_s$ and $\mu_r = 0$ seem to be reasonable approximations. Note that the Coulomb friction is just an approximation, however it is valid over a large range of parameters, but it is not accurate under all circumstances. As an overview on friction and the connected open problems, see ref. [26].

2.3. THE TANGENTIAL RESTITUTION e_t

In analogy to the normal restitution, one can define the tangential restitution e_t which is in general *not* a constant. The tangential velocity after the collision is $v_t' = -e_t v_t$. Energy conservation requires $-1 \leq e_t \leq 1$, with the two elastic extremes $e_t = -1$ and $e_t = 1$. The former corresponds to no velocity change in tangential direction, and the latter to a complete reversal. Since the tangential forces during the contact are limited by the normal force, the friction coefficient e_t depends on the impact parameter, i.e. the obliqueness of the impact.

3. Momentum conservation

In the following we will discuss the collision of two particles ($i = 1, 2$) with diameter d_i, mass m_i and velocities $\mathbf{v}_i^L = \mathbf{v}_{cm} + \mathbf{v}_i$ in the laboratory

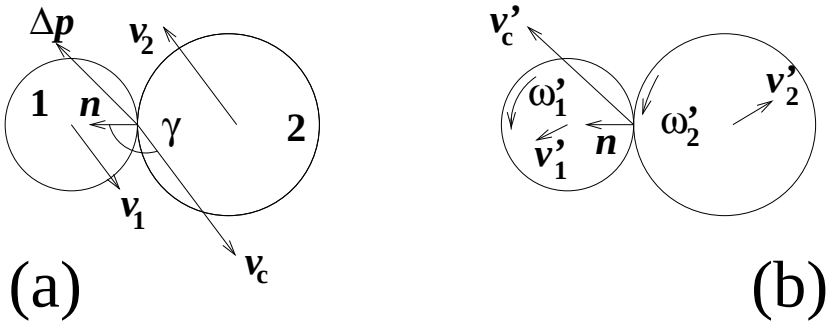

Figure 3. Schematic picture of the velocities before (a) and after (b) the collision.

reference frame. The velocity of the center of mass of these particles is

$$\mathbf{v}_{cm} = (m_1\mathbf{v}_1^L + m_2\mathbf{v}_2^L)/(m_1 + m_2). \tag{5}$$

The unit vector in normal direction [see Fig. 3] is

$$\hat{\mathbf{n}} = \frac{\mathbf{r}_1 - \mathbf{r}_2}{|\mathbf{r}_1 - \mathbf{r}_2|}, \tag{6}$$

with the position $\mathbf{r}_i$ of the center of particle i. The relative velocity of the contact-point of the particles before the collision is

$$\mathbf{v}_c = \mathbf{v}_1 - \mathbf{v}_2 - \left(\frac{d_1}{2}\omega_1 + \frac{d_2}{2}\omega_2\right) \times \hat{\mathbf{n}}, \tag{7}$$

with the linear and angular velocities $\mathbf{v}_i$ and ω_i respectively.

Note that the velocities $\mathbf{v}_1$ and $\mathbf{v}_2$ are parallel in the center of mass reference frame, which can be proven by simply calculating the vector product $\mathbf{v}_1 \times \mathbf{v}_2$. Furthermore, the change of angular momentum has the same direction for both particles.

$\mathbf{v}_c$ has the normal component $\mathbf{v}_c^{(n)} = \hat{\mathbf{n}}(\mathbf{v}_c \cdot \hat{\mathbf{n}})$ and the tangential component $\mathbf{v}_c^{(t)} = \mathbf{v}_c - \mathbf{v}_c^{(n)}$. The vector $\mathbf{v}_c^{(t)}$ defines thus the tangential unit-vector $\hat{\mathbf{t}} = \mathbf{v}_c^{(t)}/|\mathbf{v}_c^{(t)}|$. [Note that this definition of $\hat{\mathbf{t}}$ is somewhat different from the usual definition, i.e. rotating $\hat{\mathbf{n}}$ by 90 degrees in a given sense]. The collision angle γ is defined as the angle between $\hat{\mathbf{n}}$ and $\mathbf{v}_c$, and lies in the range $\pi/2 < \gamma \leq \pi$.

The conservation equations will be expressed in terms of the change of momentum $\Delta\mathbf{p}$ of particle $i = 1$. With a given force $\mathbf{f}(t)$ as a function of the time t, the change of momentum $\Delta\mathbf{p}$ is $\int_0^{t_c} \mathbf{f}(t)dt$. For vanishing contact

duration, $t_c \to 0$, or for constant forces, $\mathbf{f}(t) = const$, the nomenclature using changes of momentum $\Delta\mathbf{p}$ is equivalent to that using forces $\mathbf{f}(t)dt$.

Conservation of linear momentum requires

$$\Delta\mathbf{p} = m_1(\mathbf{v}_1' - \mathbf{v}_1) = -m_2(\mathbf{v}_2' - \mathbf{v}_2), \tag{8}$$

with the unknown velocity $\mathbf{v}_i'$ after the collision. The normal component of the change of momentum $\Delta\mathbf{p}^{(n)}$ is decoupled from the motion in the tangential direction. However, the tangential component $\Delta\mathbf{p}^{(t)}$ depends on $\Delta\mathbf{p}^{(n)}$ and causes a change of angular velocity if the surfaces are not perfectly smooth. Since $\Delta\mathbf{p}^{(t)}$ is active at the point of contact, one can calculate the change of angular momentum as the vector product between the distance vector from the center, $-(d_1/2)\hat{\mathbf{n}}$, and the change of momentum $\Delta\mathbf{p}$:

$$-\hat{\mathbf{n}} \times \Delta\mathbf{p} = \frac{2I_i}{d_i}(\omega_i' - \omega_i). \tag{9}$$

In Eq. (9), $I_i = q_i m(d_i/2)^2$ is the moment of inertia of the particle, given a rotation about its center of mass, and ω_i' is the unknown angular velocity after the collision. The prefactor in the moment of inertia is $q_i = 2/5$ for spheres and $q_i = 1/2$ for disks.

Given $\Delta\mathbf{p}$, Eqs. (8) and (9) allow the calculation of all unknown velocities after the collision:

$$\mathbf{v}_1' = \mathbf{v}_1 + \Delta\mathbf{p}/m_1, \tag{10}$$

$$\omega_1' = \omega_1 - \frac{d_1}{(2I_1)}\hat{\mathbf{n}} \times \Delta\mathbf{p}, \tag{11}$$

$$\mathbf{v}_2' = \mathbf{v}_2 - \Delta\mathbf{p}/m_2, \text{ and} \tag{12}$$

$$\omega_2' = \omega_2 - \frac{d_2}{(2I_2)}\hat{\mathbf{n}} \times \Delta\mathbf{p}. \tag{13}$$

The fact that the change of angular momentum is the same for both particles results in a change of the collision angle from γ to γ'. A measure for the obliqueness of an impact is the impact parameter

$$\mathbf{b} = (\mathbf{r}_1 - \mathbf{r}_2) \times \frac{\mathbf{v}_1 - \mathbf{v}_2}{|\mathbf{v}_1 - \mathbf{v}_2|}. \tag{14}$$

In the simple case of identical particles, the point of contact is identical to the center of mass, so that the total angular momentum $\mathbf{L}_{\text{tot}}$ is conserved and has components due to the spin and to the obliqueness of the impact:

$$\mathbf{L}_{\text{tot}} = I(\omega_1+\omega_2)+\frac{m}{2}\mathbf{b}|\mathbf{v}_1-\mathbf{v}_2| = \frac{mqd^2}{4}(\omega_1+\omega_2)+\frac{m}{2}(\mathbf{r}_1-\mathbf{r}_2)\times(\mathbf{v}_1-\mathbf{v}_2). \tag{15}$$

Since the particles were assumed to be identical, we used $d = d_1 = d_2$, $m = m_1 = m_2$ and $I = qm(d/2)^2$.

4. The change of momentum $\Delta\mathbf{p}$

In order to calculate the velocities after a collision from Eqs.(10-13), only the change of momentum $\Delta\mathbf{p}$ has to be known. The normal component is calculated using the definition of the restitution coefficient in Eq. (1). Inserting Eqs. (10) and (12) The normal component of the difference in the change of velocities is $\Delta\mathbf{v}^{(n)} = \mathbf{v}_1^{(n)} - \mathbf{v}_2^{(n)} = \Delta\mathbf{p}^{(n)}/m_1 + \Delta\mathbf{p}^{(n)}/m_2$. Inserting Eqs. (10) and (12) into $\Delta\mathbf{v}^{(n)}$ gives the momentum change in the normal direction

$$\Delta\mathbf{p}^{(n)} = -m_{12}(1+e_n)\mathbf{v}_c^{(n)}, \tag{16}$$

with the reduced mass $m_{12} = m_1 m_2/(m_1+m_2)$.

4.1. COULOMB FRICTION AND TANGENTIAL ELASTICITY

Coulomb's law connects the normal and the tangential force at a contact. An alternative interpretation connects the components of the change of momentum in the corresponding directions: $|\Delta\mathbf{p}^{(t)}| \leq \mu|\Delta\mathbf{p}^{(n)}|$, with $\mu \geq 0$. Since friction is active in the direction opposite to the relative velocity $\mathbf{v}_c^{(t)}$, the change of momentum $\Delta\mathbf{p}^{(t)}$ is parallel to $-\hat{\mathbf{t}}$. Thus we have the inequality

$$\Delta\mathbf{p}^{(t)} \leq \mu m_{12}(1+e_n)v_c\cos(\gamma)\ \hat{\mathbf{t}}\ . \tag{17}$$

Using $v_c^{(n)} = |\mathbf{v}_c^{(n)}| = -v_c\cos(\gamma)$ [since $\cos(\gamma) \leq 0$ for all possible γ] and $\hat{\mathbf{t}} = \mathbf{v}_c^{(t)}/(v_c\sin\gamma)$, we have the tangential component of the change of momentum for a contact that follows Coulomb's law:

$$\Delta\mathbf{p}^{(t)} = m_{12}\mu(1+e_n)\cot(\gamma)\ \mathbf{v}_c^{(t)}. \tag{18}$$

In the limit $\gamma \to \pi$ one has $\cot(\gamma) \to -\infty$, and $\gamma = \pi$ corresponds to a central collision. In this case of extremely small tangential velocities, $\Delta\mathbf{p}^{(t)}$ in Eq. (18) may get very large. A large change of momentum may result in a gain of energy and thus has to be avoided. The validity of the above equation is the range of sliding contacts. As soon as the tangential velocity gets too small, other assumptions are needed in order to calculate the change of momentum in the tangential direction. In order to avoid the gain of energy, Walton and Braun proposed a cut-off, i.e. a coefficient of maximum tangential restitution e_{t0} [1]. Limiting this coefficient to $-1 \leq e_{t0} \leq 1$ allows the calculation of $\Delta\mathbf{p}$ for all possible values of γ. The change of momentum

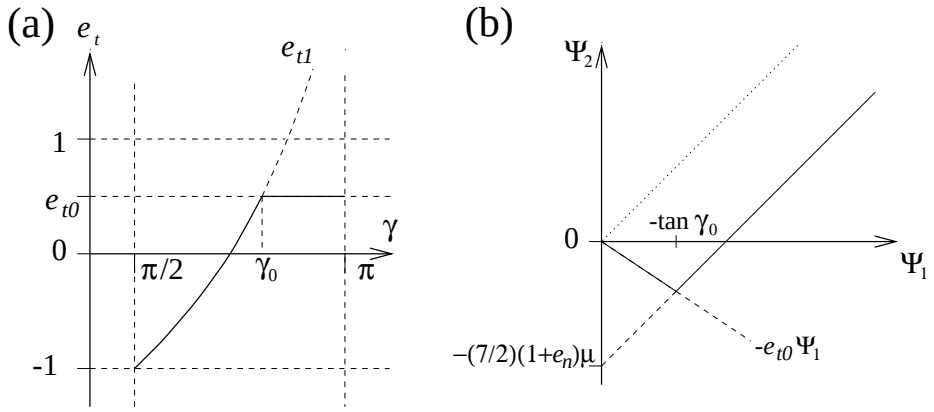

Figure 4. (a) e_t as a function of γ. (b) $\Psi_2 = v_c'^{(t)}/v_c^{(n)}$ as function of $\Psi_1 = v_c^{(t)}/v_c^{(n)}$.

of particle $i = 1$ is thus

$$\Delta \mathbf{p} = -m_{12}(1+e_n)\mathbf{v}_c^{(n)} - m_{12}\left(\frac{q}{1+q}\right)(1+e_t)\mathbf{v}_c^{(t)}, \tag{19}$$

with the normal and tangential restitution e_n and e_t appearing in a similar form. The factor $q/(1+q)$ stems from the change of angular momentum. The tangential restitution in Eq. (19) is $e_t = \min[e_{t0}, e_{t1}]$. For small γ, i.e. grazing collisions, one has $e_t = e_{t1}$, whereas for large γ, i.e. central collisions, one has $e_t = e_{t0}$. Note that inserting the tangential restitution

$$e_{t1} = -1 - \mu(1+e_n)\cot(\gamma)\left(1+\frac{1}{q}\right) \tag{20}$$

into Eq. (19), leads back to Eq. (18). In Fig. 4(a) the tangential restitution e_t is shown as a function of the angle of the collision γ.

4.2. MEASUREMENT AND CLASSIFICATION OF COLLISIONS

For a quantitative classification of collisions, different authors [3, 11, 23] used the ratio of tangential and normal velocity, introduced first by Mindlin [12], Mindlin and Deresiewicz [13] and Maw, Barber, and Fawcett [14, 15]. Before the collision one has $\Psi_1 = v_c^{(t)}/v_c^{(n)} = -\tan\gamma$, and after the collision one has $\Psi_2 = v_c'^{(t)}/v_c^{(n)} = e_n \tan\gamma'$. Here, γ' is the angle between $\mathbf{v_c'}$ and $\hat{\mathbf{n}}$. From Eq. (19) one gets

$$\Psi_2 = \begin{cases} \Psi_1 - \frac{1+q}{q}(1+e_n)\mu & \text{for } \gamma < \gamma_0 \\ -e_{t0}\Psi_1 & \text{for } \gamma \geq \gamma_0. \end{cases} \tag{21}$$

In Fig. 4(b) the behavior of Ψ_2 as function of Ψ_1 is plotted schematically. The dotted line corresponds to perfectly smooth particles, i.e. $\mu = 0$, and the solid line represents Eq. (21). Experiments [11, 16] show that, within fluctuations, every collision can be fitted by Eq. (21) reasonably well. Note that the measurements lead typically to positive values of e_{t0}, corresponding to an inversion of the tangential velocity for central collisions. This inversion is caused by the elasticity of the material which is important in the case of sticking contacts rather than the case of sliding contacts [see the chapter by S. Roux in this book].

5. The integration of a two-particle contact

Replacing $\Delta\mathbf{p}$ by $\mathbf{f}(t)\Delta t$, and assuming $\Delta t = dt$ to be infinitesimally small, one gets differential equations for the change of the velocities of the particles $dv = v' - v$ and $d\omega = \omega' - \omega$. In the following, we solve the differential equations for some simple cases. In contrast to the above discussion, the particles are assumed to be deformable.

Therefore we define, as a measure for the deformation, the overlap

$$\delta = \frac{1}{2}(d_1 + d_2) - (\mathbf{r}_1 - \mathbf{r}_2)\hat{\mathbf{n}}, \tag{22}$$

and the relative tangential velocity of the particles' surfaces

$$\frac{d}{dt}\vartheta = \mathbf{v}_c\hat{\mathbf{t}}, \tag{23}$$

with the tangential displacement ϑ. Note that $\frac{d}{dt}\delta = \dot{\delta} = -\mathbf{v}_c\hat{\mathbf{n}}$ is positive before and negative after the collision, whereas $\dot{\vartheta} = \mathbf{v}_c\hat{\mathbf{t}}$ is always positive, due to the definition of $\hat{\mathbf{t}}$.

Since $\ddot{\delta} = \frac{d^2}{dt^2}\delta = -\frac{d}{dt}\mathbf{v}_c\hat{\mathbf{n}}$ one gets $\ddot{\delta} = -f_1^{(n)}/m_1 + f_2^{(n)}/m_2$, where $f_i^{(n)} = m_i\ddot{\mathbf{r}}_i\hat{\mathbf{n}}$ is the force acting in normal direction on particle i. Newton's third law of motion leads to $f_2^{(n)} = -f_1^{(n)}$, and thus the change of normal velocity

$$\ddot{\delta} = -\frac{d}{dt}\mathbf{v}_c\hat{\mathbf{n}} = -\frac{1}{m_{12}}f_1^{(n)}. \tag{24}$$

This differential equation in δ can be solved for simple forces $f_1^{(n)}(\delta, \dot{\delta}, t)$ [22], and thus allows the analytical description of the particle trajectory in the normal direction.

In the tangential direction one can calculate a similar differential equation from Eqs. (10-13) and (23):

$$\ddot{\vartheta} = \frac{d}{dt}\mathbf{v}_c\hat{\mathbf{t}} = \frac{1}{m_{12}}\left(1 + \frac{1}{q}\right)f_1^{(t)}. \tag{25}$$

For spheres the moment of inertia is $I_i = q_i m_i (d_i/2)^2$ with $q_i = 2/5$. The double cross product $[\hat{\mathbf{n}} \times \mathbf{f}_1^{(t)}] \times \hat{\mathbf{n}}$, that occurs during the calculation of Eq. (25), can be reduced to $f_1^{(t)}$. Also Eq. (25) can be solved for simple forces $f_1^{(t)}$ as we will show in the following.

The knowledge of the forces $f_1^{(n)}$ and $f_1^{(t)}$ is the condition for the solution of the equations of motion. For the forces in the normal direction, older experiments exist [7], but exact measurements of the force in tangential direction are rare. Usually one measures just the velocities before and after the collision and calculates the corresponding change in momentum to be inserted in the Eqs. (10-13). As we will recognize in the following, the knowledge of $\Delta\mathbf{p}$ does not necessarily allow a unique choice of the force, since different forces may lead to the same $\Delta\mathbf{p}$. The following calculations will clarify how far the choice of the force laws has an influence on the contact duration and the restitution coefficients and thus on the dynamics of the collision.

6. Models for the repulsive potential

In order to model 'hard' particles that interact on contact, a repulsive potential is required. The repulsive force is of short range and depends e.g. on the Young modulus and the Poisson ratio of the material, and on the shape of the particle as well. These quantities determine also the duration of a contact t_c. The simplest linear approach consists of a spring with stiffness k, a more advanced approach is connected to the Hertz theory of elastic spheres [27] and involves a displacement dependent spring constant $k \propto \delta^{1/2}$, and thus a nonlinear force $f^{(n)} \propto \delta^{3/2}$.

6.1. THE LINEAR SPRING-DASHPOT MODEL (LSD)

In the simplest approximation, the force acting on particle $i = 1$ is a linear spring with spring constant k, so that the repulsive normal force is

$$f_{el}^{(n)} = k\delta, \tag{26}$$

active only when the overlap is positive ($\delta \geq 0$). In order to introduce dissipation into the system, one assumes a viscous damping, i.e. velocity dependent, directed opposite to $\mathbf{v}_c^{(n)}$, so that

$$f_{diss}^{(n)} = \nu_n \dot{\delta}. \tag{27}$$

Inserting Eqs. (26) and (27) into Eq. (24) one gets the well-known differential equation of the damped harmonic oscillator

$$\ddot{\delta} + 2\eta\dot{\delta} + \omega_0^2\delta = 0. \tag{28}$$

In Eq. (28) we have defined the oscillation frequency of an elastic oscillator $\omega_0 = \sqrt{k/m_{12}}$, and the effective viscosity $\eta = \nu_n/(2m_{12})$. The solution of Eq. (28) is

$$\delta(t) \;=\; (v_0/\omega)\;\exp(-\eta t)\;\sin(\omega t) \tag{29}$$

with the velocity

$$\dot{\delta}(t) \;=\; (v_0/\omega)\;\exp(-\eta t)\;\left[-\eta\;\sin(\omega t) + \omega\;\cos(\omega t)\;\right]. \tag{30}$$

In Eqs. (29) and (30) we use the initial relative velocity $v_0 = \dot{\delta}(0)$ and the oscillation frequency of the damped oscillator $\omega = \sqrt{\omega_0^2 - \eta^2}$. As long as $\eta < \omega_0$ the duration of a contact is

$$t_c = \pi/\omega, \tag{31}$$

i.e. the half period of oscillation, since the contact is assumed to end as soon as δ gets negative $\delta(t) < 0$. From Eq. (1) we calculate the coefficient of restitution

$$e_n = \exp(-\pi\eta/\omega), \tag{32}$$

and the maximum overlap $\delta_{\max}$ at time $t_{\max}$ from the condition $\dot{\delta}(t_{\max}) = 0$, i.e. $\omega t_{\max} = \arctan(\omega/\eta) = \arcsin(\omega/\omega_0)$. Thus we get

$$\begin{aligned} \delta_{\max} &= (v_0/\omega)\exp(-\eta t_{\max})\sin(\omega t_{\max}) && (33)\\ &= (v_0/\omega_0)\exp\left[(-\eta/\omega)\arcsin(\omega/\omega_0)\right]. && (34) \end{aligned}$$

As we will proceed to show, the rule $\delta(t_c) = 0$ is *not* appropriate to decide when the contact of non-cohesive particles ends. Already for weak dissipation, the force at time t_c is attractive !

In Fig. 5(a) we present the normal component of the force acting on one particle during a collision. We observe that the force has a finite value at the beginning of the contact $t = 0$ due to the viscous damping term. With increasing viscosity the force becomes negative for times shorter than t_c.

The convenient rule to decide when the contact ends should thus be the condition $f_1^{(n)}(t_c^f) = 0$, with the duration of the contact t_c^f, defined through that force rule. Inserting Eqs. (29) and (30) into this rule, we have

$$0 = \left(\frac{v_0}{\omega}\right)\;\exp(-\eta t_c^f)\;\left[(k - 2m_{12}\eta^2)\;\sin(\omega t_c^f) + 2m_{12}\eta\omega\;\cos(\omega t_c^f)\;\right], \tag{35}$$

with the solution

$$t_c^f = \frac{1}{\omega}\left(\pi - \arctan\frac{2\eta\omega}{\omega^2 - \eta^2}\right) = \frac{1}{\omega}\left(\pi - 2\arctan\frac{\eta}{\omega}\right). \tag{36}$$

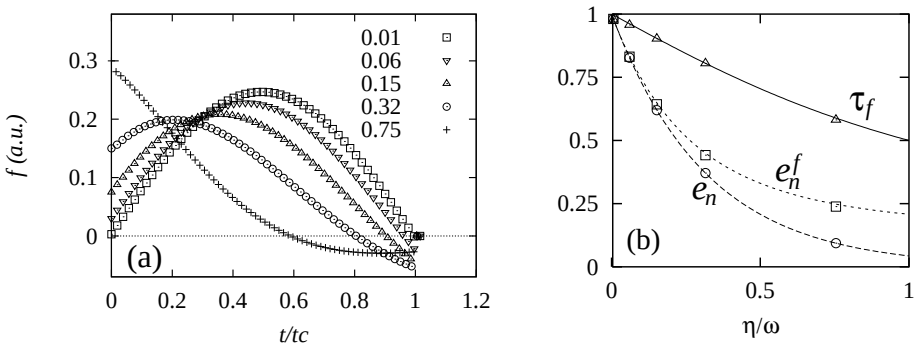

Figure 5. (a) Normal force in arbitrary units as a function of time (scaled by t_c) for different η/ω given as insert. (b) The ratio $\tau_f = t_c^f/t_c$ and the restitution coefficients e_n and e_n^f as a functions of the strengh of inelasticity η/ω. The lines correspond to the analytical expressions and the data points correspond to the numerical solution in (a).

The last transformation is an addition-theorem for $(\eta/\omega)^2 < 1$ and the solution is thus valid in the interval $-\pi/2 < \omega t_c^f < 3\pi/2$. Only in the elastic limit, where $\eta = 0$ and $\omega = \omega_0$, is the contact duration following from both definitions equivalent. For $\omega > \eta > 0$ we have the ratio $\tau_f = t_c^f/t_c$ different from unity. Since t_c^f is always smaller than t_c we have $\tau_f < 1$, however, for weak to intermediate dissipation strength the value of τ_f is close to unity, i.e. the difference between the definitions is rather small. For stronger dissipation, the second definition has to be chosen, since it explicitly excludes attractive forces. In Fig. 5(b) we present the ratio τ_f and the restitution coefficients $e_n = \exp(-\eta t_c)$ and $e_n^f = \exp(-\eta t_c^f)$ as functions of η/ω.

6.2. A GENERAL, NONLINEAR SPRING-DASHPOT MODEL

Instead of a linear spring, see Eq. (26), we propose a more general nonlinear force

$$f_\alpha^{(n)} = Yd^2 \left(\frac{\delta}{d}\right)^{1+\alpha}, \tag{37}$$

with the effective particle diameter $d = (2d_1d_2)/(d_1 + d_2)$, the effective, geometry dependent stiffness $Y^{-1} = \frac{3}{2}\left(\frac{1-\sigma_1^2}{E_1} + \frac{1-\sigma_2^2}{E_2}\right)$, and thus the spring constant $k(\delta) = Yd(\delta/d)^\alpha$. Here σ_i is the Poisson ratio and E_i is the Young modulus of the material that particle i consists of. In the case $\alpha = 0$ we obtain Eq. (26) again, and in the case $\alpha = 1/2$ we have the Hertz contact [22, 27, 28].

Modelling dissipation for a more general repulsive force may require also a more general dissipative force

$$f^{(n)}_{\zeta_0,\zeta_1} = \eta d\dot{\delta} \left(\frac{\delta}{d}\right)^{\zeta_0} \left(\frac{\dot{\delta}}{\dot{\delta}_0}\right)^{\zeta_1} \tag{38}$$

with an effective viscosity η and a typical velocity scale $\dot{\delta}_0$.

The exact calculation of the contact duration t_c is possible in the limit of vanishing dissipation only, i.e. $\eta = 0$. A more elaborate calculation is performed in ref. [24]. The maximum overlap $\delta_{\max}$ is achieved with the condition $\dot{\delta} = 0$ from the energy conservation equation $E_k(t) + E_p(t) = E_k(0)$, with the kinetic energy E_k and the potential energy due to the repulsive interaction E_p. The initial values are $E_k = m_{12}v_0^2/2$ and $E_p = 0$. The kinetic energy is completely transferred to potential energy $E_p = Yd^{1-\alpha}\delta_{\max}^{2+\alpha}/(2+\alpha)$, so that

$$\delta_{\max} = \left(1 + \frac{\alpha}{2}\right)^{1/(2+\alpha)} \left(\frac{m_{12}}{Yd^{1-\alpha}}\right)^{1/(2+\alpha)} v_0^{2/(2+\alpha)}. \tag{39}$$

The separation of variables δ and t in the energy conservation equation leads to the half contact duration $t_c/2$ as integral from $\delta = 0$ to $\delta = \delta_{\max}$, so that

$$t_c = J(\alpha)\frac{\delta_{\max}}{v_0} = J(\alpha) \left(1 + \frac{\alpha}{2}\right)^{1/(2+\alpha)} \left(\frac{m_{12}}{Yd^{1-\alpha}}\right)^{1/(2+\alpha)} v_0^{-\alpha/(2+\alpha)}. \tag{40}$$

The function

$$J(\alpha) = \frac{\sqrt{\pi}\Gamma(\frac{1}{2+\alpha})}{(1+\frac{\alpha}{2})\Gamma(\frac{4+\alpha}{4+2\alpha})} \tag{41}$$

contains the Gamma function $\Gamma(x)$, so that $J(0) = \pi$ and $J(1/2) = 2.94$ are the prefactors in Eq. (40). Note that the contact duration for $\alpha \neq 0$ depends on the initial relative velocity, i.e. $t_c \propto v_0^{-\alpha/(2+\alpha)}$. With increasing relative velocity the contact duration decreases.

An estimate for the restitution coefficient in the limit of weak dissipation requires the simplifying assumption that the dissipated energy is proportional to the dissipative force $f^{(n)}_{\zeta_0,\zeta_1}$ and proportional to the distance $\delta_{\max}$ on which the force was active. The dissipated energy is thus

$$E_{\text{diss}} \propto f^{(n)}_{\zeta_0,\zeta_1}\delta_{\max} = \eta d^{1-\zeta_0}\delta_{\max}^{1+\zeta_0}v_0^{1+\zeta_1} \propto v_0^{\frac{4+2(\zeta_0+\zeta_1)+\alpha(1+\zeta_1)}{2+\alpha}}, \tag{42}$$

what leads to the velocity dependence of the restitution coefficient

$$1 - e_n \propto v_0^{\frac{2(\zeta_0+\zeta_1)-\alpha(1-\zeta_1)}{2+\alpha}}. \tag{43}$$

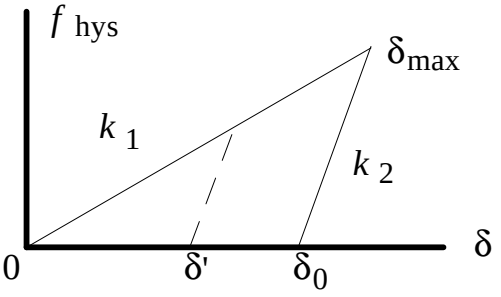

Figure 6. Schematic drawing of the hysteretic repulsive force law in Eq. (45). During the first loading, $f_{\rm hys}$ follows the path $0 \to \delta_{\rm max}$, and during unloading it follows the path $\delta_{\rm max} \to \delta_0$. A reloading before the overlap dropped to zero may take plase e.g. at δ', from where $f_{\rm hys}$ follows the dashed line up the the path of initial loading.

For $\alpha = 1/2$, $\zeta_0 = 1/2$, and $\zeta_1 = 0$ one gets $1 - e_n \propto v_0^{1/5}$ [22, 24, 29, 30]. Inserting into Eq. (37) the identity $\dot{\delta}_0 = v_0$, the nonlinear terms with the exponent ζ_1 dissappear and one gets

$$1 - e_n \propto v_0^{\frac{2\zeta_0 - \alpha}{2+\alpha}}. \tag{44}$$

In order to get a velocity independent restitution coefficient the condition $2(\zeta_0+\zeta_1)+\alpha(\zeta_1-1) = 0$ has to be fulfilled. For Hertz contacts with $\alpha = 1/2$ this leads to the rule $4\zeta_0 + 5\zeta_1 = 1$ [30].

6.3. A HYSTERETIC SPRING MODEL

Instead of viscous dissipation, one observes also permanent, plastic deformation during a typical collision. Therefore, an alternative to the simple linear model in subsection 6.1, and to the more complicated nonlinear model in subsection 6.2, is a hysteretic force-overlap relation accounting for permanent deformations. Instead of more realistic, but much more complicated nonlinear-hysteretic force laws [1, 31, 32], we present here only the linear-hysteretic model [1]. For loading a weaker spring is used as for unloading, so that the repulsive force can be written as

$$f_{\rm hys}^{(n)} = \begin{cases} k_1\delta & \text{for loading, and} \\ k_2(\delta - \delta_0) & \text{for unloading,} \end{cases} \tag{45}$$

with $k_1 < k_2$. This repulsive force is shown in Fig. 6.

During the initial loading the force increases linearly with the overlap δ and the spring constant k_1 until the maximum overlap $\delta_{\rm max}$ is reached. During unloading the force drops to zero at overlap δ_0 that can be calculated from the continuity of the force $k_1\delta_{\rm max} = k_2(\delta_{\rm max} - \delta_0)$. The contact

duration

$$t_c = \frac{\pi}{2\omega_1} + \frac{\pi}{2\omega_2} = \frac{\pi}{2}\left(\sqrt{\frac{m_{12}}{k_1}} + \sqrt{\frac{m_{12}}{k_2}}\right) \tag{46}$$

follows from Eq. (31) as sum of the half contact duration of particles with either stiffness k_1 and k_2. The dissipated energy may be identified as the surface within the path $0 \to \delta_{\max} \to \delta_0 \to 0$, and leads to the restitution coefficient

$$e_n = \sqrt{\frac{k_1}{k_2}}. \tag{47}$$

The contact ends as soon as the force vanishes at overlap δ_0, however, the overlap vanishes later at time $t_c + \delta_0/v(t_c)$, since the particles separate with velocity $v(t_c) = e_n v_0$. After a complete separation, the plastic deformation is neglected, one assumes that the particle does not collide again at exactly the same point and thus the new contact point should be not yet deformed. If a new contact happens before the particles could separate, the loading follows the steep path $k_2(\delta - \delta')$ until the path of initial loading is reached. Given e_n and t_c the two spring constants can be calculated easily, i.e. $k_1 = m_{12}\pi^2(1 + e_n^2)/(4t_c^2)$ and $k_2 = k_1/e_n$.

The advantage of this model is that no arbitrary viscosity has to be included and that the parameters e_n and t_c can be predicted analytically. However, neither this model nor one of the models above represent the full experimental reality.

7. Modeling tangential forces

In the following we will use the linear spring-dashpot model in normal direction, i.e. $\alpha = \zeta_0 = \zeta_1 = 0$, and try three simple tangential force laws. We will apply the laws one by one, however, a combination is possible.

7.1. VISCOUS TANGENTIAL FORCE

The by far simplest tangential force is a viscous friction

$$f_\nu^{(t)} = -\nu_t \dot{\vartheta}, \tag{48}$$

with a tangential viscosity ν_t. The tangential component of the relative velocity is $\dot{\vartheta}$. Inserting Eq. (48) into Eq. (25) and integrating from $t = 0$ to $t = t_c$ leads to the tangential velocity at the end of the contact

$$v_c'^{(t)} = v_c^{(t)} \exp(-2\eta_t t_c), \tag{49}$$

with $\eta_t = \left(1 + \frac{1}{q}\right)\nu_t/(2m_{12})$ in analogy to the viscosity η. Inserting $v_c'^{(t)}$ into the definition of Ψ_2 leads to

$$\Psi_2 = \Psi_1 \exp(-2\eta_t t_c). \tag{50}$$

Thus the viscous tangential force leads to a reduction of the relative tangential velocity of the points of contact. This corresponds to the range of tangential restitution $-1 \leq e_t \leq 0$. The application of a viscous tangential force makes sense only for collision angles $\gamma \geq \gamma_0$ [see Eq. (21)], but cannot lead to a positive e_t.

7.2. COULOMB FRICTION FORCE

During the contact, the tangential force is coupled to the normal force via

$$f^{(t)} = -\mu f^{(n)}, \tag{51}$$

and it is directed opposite to the tangential velocity. The calculation of the tangential velocity during the contact thus requires the knowledge of the normal force at each time during the contact. The integration of the changes in velocity lead to

$$v_c'^{(t)} = v_c^{(t)} + \mu \left(1 + \frac{1}{q}\right) (1 + e_n) v_c^{(n)}. \tag{52}$$

After division of $v_c'^{(t)}$ by $v_c^{(n)}$ we obtain $\Psi_2(\gamma < \gamma_0)$ as in Eq. (21). Note that during the integration of the force law in Eq. (51) the velocity may drop to zero. In that case the direction $\hat{\mathbf{t}}$ is ill-defined and the velocity stays zero. The discrete numerical integration instead may lead to spurious oscillations around $v_c^{(t)} = 0$.

7.3. ELASTIC TANGENTIAL SPRING

For negative e_{t0} the combination of the above presented force laws allows a reasonable modeling of the contact in the tangential direction. However, since most materials have a positive e_{t0} [11], one has to come up with a tangential force that allows the inversion of the tangential velocity. A possible inversion is connected to the elasticity of the material, i.e. parts of the contact area store elastic energy and release it before the contact ends. In order to account for material elasticity a tangential spring was proposed [1, 14, 15] similar to the spring in normal direction.

In analogy to the linear spring in normal direction we define

$$f^{(t)} = -k_t \vartheta, \tag{53}$$

insert it into Eq. (25) and get for an infinitesimal change of velocity

$$d\dot{\vartheta} = -\frac{1}{m_{12}} \left(1 + \frac{1}{q}\right) k_t \vartheta(t) dt. \tag{54}$$

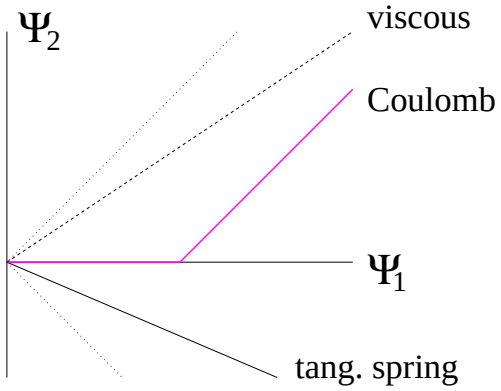

Figure 7. Schematic picture of the velocity ratio Ψ_2 versus Ψ_1 for the different force laws in Eq. (48) (dashed line), Eq. (51) (thick grey line), and Eq. (53) (thin solid line). The dotted lines denote the limits $\mu = 0$ (top, slope 1) and $\mu = \infty$, $e_{t0} = 1$ (bottom, with slope -1).

Using the Ansatz $\vartheta(t) = (v_c^{(t)}/\omega_t)\sin(\omega_t t)$, substituting $\omega_t^2 = (k_t/m_{12})(1 + 1/q)$, and integrating over the contact duration we arrive at

$$v_c'^{(t)} = v_c^{(t)}\cos(\omega_t t_c). \tag{55}$$

Dividing $v_c'^{(t)}$ by $v_c^{(n)}$ we get again $\Psi_2(\gamma \geq \gamma_0)$ from Eq. (21). Now, a positive tangential restitution with $e_{t0} = -\cos(\pi\omega_t/\omega)$ is possible. Given a certain value of e_{t0} [typically $e_{t0} \approx 0.5$ is found from experiments [11]], we have a rule for the choice of the tangential spring:

$$\omega_t = \sqrt{\frac{k_t}{m_{12}}\left(\frac{1+q}{q}\right)} = \frac{1}{t_c}\arccos(-e_{t0}) \tag{56}$$

and thus the ratio of tangential and normal spring-stiffness

$$\frac{k_t}{k} = \frac{q}{1+q}\left(\frac{\arccos(-e_{t0})}{\pi}\right)^2. \tag{57}$$

7.4. A CLASSIFICATION OF THE TANGENTIAL FORCE LAWS

In Fig. 7 we plot schematically the results obtained with the different force laws. Note that the negative slope of Ψ_2, i.e. the physical behavior, can be found only for the tangential spring force law in Eq. (53).

The combination of the tangential spring (for $\gamma < \gamma_0$) and the Coulomb friction (for $\gamma \geq \gamma_0$) leads now to the desired Ψ_2 as also found in experiments. In order to learn how this combination is practically carried out in

numerical simulations see ref. [23] or the contribution by L. Brendel to this book.

8. Summary and Conclusion

In this chapter we discussed two-particle contacts and introduced the three parameters: restitution coefficient, friction coefficient, and maximum tangential restitution. The first accounts for the normal direction, whereas the latter two account for the tangential direction. These three parameters suffice to classify those collisions which have been measured experimentally. Despite the fact that this three-parameter model includes simplifications, such as the exclusive occurence of either sliding or sticking contacts, it is a reasonable and simple model.

In the normal direction we performed the more elaborate integration of the equations of motion, using linear, non-linear, and hysteretic interactions. Dissipative effects like viscosity or plastic deformations are described by the coefficient of restitution e_n that e.g. depends on the velocity of impact [22–24]. Since this dependence is usually very weak, a constant e_n is often a good approximation.

In the tangential direction one has to distinguish between sliding and sticking contacts, the first type follows Coulomb's friction law with the coefficient of friction μ, whereas the latter can be modeled by a tangential spring and may lead to a positive e_t. In the three parameter model, a contact is either sliding or sticking, even when a real contact is much more complicated [see the chapter by S. Roux in this book].

Two possibilities to model a collision of two particles were described. In the "hard" particle model only the three parameters are used and the contact is assumed to happen instantaneously. In the "soft" particle model the equations of motion are solved for the two particles, however, the choice of normal and tangential forces is required. Note that different forces may lead to the same result, i.e. the same three parameters. In the case of two-particle contacts the choice of the force law and even the choice of the collision model is not important. Thus one has almost free choice for dilute systems where almost all collisions are binary [33]. In the case of a denser system, where contacts may be permanent and one particle has often more than one contact partner, the choice of the interaction model influences the behavior of the system [22, 34, 35].

As a rule, one should compare the interaction model used with experimental data, and one should try to get as close as possible to the experimental results. However, measurements exist only for a small range in parameter space, and – to my knowledge – no systematic experiments exist for multi-particle contacts (pool billard is an adequate laboratory for this

purpose). Thus we propose to choose the simplest model, which still fits the existing experimental data reasonably well.

Acknowledgements. Thanks to S. Weinketz and B. Wachmann for proofreading, and S. McNamara and T. Shinbrot for helpful comments. The DFG, SFB 382 is acknowledged for financial support.

References

1. O. R. Walton and R.L. Braun. Viscosity, granular-temperature, and stress calculations for shearing assemblies of inelastic, frictional disks. *Journal of Rheology*, 30(5):949–980, 1986.
2. M. P. Allen and D. J. Tildesley. *Computer Simulation of Liquids*. Oxford University Press, Oxford, 1987.
3. S. Luding. Granular materials under vibration: Simulations of rotating spheres. *Phys. Rev. E*, 52(4):4442, 1995.
4. O. M. Rayleigh. On the production of vibrations by forces of relatively long duration, with application to the theory of collisions. *Phil. Mag. Series 6*, 11:283–291, 1906.
5. C. V. Raman. The photographic study of impact at minimal velocities. *Phys. Rev.*, 12:442–447, 1918.
6. L. J. Briggs. Methods for measuring the coefficient of restitution and the spin of a ball. *J. of Research of the National Bureau of Standards*, 34:1–23, 1945.
7. W. Goldsmith. *IMPACT, The theory and physical behavior of colliding solids*. Edward Arnold, London, 1964.
8. J. Reed. Energy losses due to elastic wave propagation during an elastic impact. *J. Phys. D*, 18:2329, 1985.
9. R. Sondergaard, K. Chaney, and C.E. Brennen. Measurements of solid spheres bouncing off flat plates. *Journal of Applied Mechanics*, 57:694–699, 1990.
10. R. N. Dave, J. Yu, and A. D. Rosato. Measurement of collisional properties of spheres using high-speed video analysis. preprint, 1994.
11. S. F. Foerster, M. Y. Louge, H. Chang, and K. Allia. Measurements of the collision properties of small spheres. *Phys. Fluids*, 6(3):1108–1115, 1994.
12. R. D. Mindlin. Compliance of elastic bodies in contact. *J. of Appl. Mech.*, 16:259, 1949.
13. R. D. Mindlin and H. Deresiewicz. Elastic spheres in contact under varying oblique forces. *J. of Appl. Mech.*, 20:327, 1953.
14. N. Maw, J. R. Barber, and J. N. Fawcett. The oblique impact of elastic spheres. *Wear*, 38:101, 1976.
15. N. Maw, J. R. Barber, and J. N. Fawcett. The role of elastic tangential compliance in oblique impact. *J. Lubrication Tech.*, 103:74, 1981.
16. L. Labous, A. D. Rosato, and R. Dave. Measurements of collision properties of spheres using high-speed video analysis. , 1997.
17. J. Duran, T. Mazozi, S. Luding, E. Clément, and J. Rajchenbach. Discontinuous decompaction of a falling sandpile. *Phys. Rev. E*, 53(2):1923, 1996.
18. S. Luding, J. Duran, T. Mazozi, E. Clément, and J. Rajchenbach. Simulations of granular flow: Cracks in a falling sandpile. In D. E. Wolf, M. Schreckenberg, and A. Bachem, editors, *Traffic and Granular Flow*, Singapore, 1996. World Scientific.
19. S. Luding, J. Duran, E. Clément, and J. Rajchenbach. Simulations of dense granular flow: Dynamic arches and spin organization. *J. Phys. I France*, 6:823–836, 1996.
20. S. Luding, J. Duran, E. Clément, and J. Rajchenbach. Computer simulations and experiments of dry granular media: Polydisperse disks in a vertical pipe. In *Proc. of the 5th Chemical Engineering World Congress*, San Diego, 1996. AIChE.
21. S. Luding, E. Clément, J. Rajchenbach, and J. Duran. Simulations of pattern formation in vibrated granular media. *Europhys. Lett.*, 36(4):247–252, 1996.

22. S. Luding, E. Clément, A. Blumen, J. Rajchenbach, and J. Duran. Anomalous energy dissipation in molecular dynamics simulations of grains: The "detachment effect". *Phys. Rev. E*, 50:4113, 1994.
23. J. Schäfer, S. Dippel, and D. E. Wolf. Force schemes in simulations of granular materials. *J.Phys. I France*, 6:5–20, 1996.
24. N. V. Brilliantov, F. Spahn, J. M. Hertzsch, and T. Pöschel. Model for collisions in granular gases. *Phys. Rev. E*, 53(5):5382, 1996.
25. M. Coulomb. Theorie des Machines Simples. *Academie des Sciences*, 10:166, 1781.
26. D. E. Wolf and P. Grassberger, editors. *Friction, Arching and Contact Dynamics*. World Scientific, Singapore, 1997.
27. H. Hertz. Über die Berührung fester elastischer Körper. *J. für die reine u. angew. Math.*, 92:136, 1882.
28. L. D. Landau and E. M. Lifschitz. *Elastizit"atstheorie*. Akademie Verlag Dresden, Berlin, 1989.
29. G. Kuwabara and K. Kono. Restitution coefficient in a collision between two spheres. *Japanese Journal of Applied Physics*, 26(8):1230–1233, 1987.
30. Y.-h. Taguchi. Numerical modelling of convective motion in granular materials. In S. Kai, editor, *Pattern Formation in Complex Dissipative Systems*, page 341, Singapore, 1991. World Scientific.
31. C. Y. Zhu, A. Shukla, and M. H. Sadd. Prediction of dynamic contact loads in granular assemblies. *J. of Applied Mechanics*, 58:341, 1991.
32. M. H. Sadd, Q. M. Tai, and A. Shukla. Contact law effects on wave propagation in particulate materials using distinct element modeling. *Int. J. Non-Linear Mechanics*, 28(2):251, 1993.
33. S. Luding, H. J. Herrmann, and A. Blumen. Scaling behavior of 2-dimensional arrays of beads under external vibrations. *Phys. Rev. E*, 50:3100, 1994.
34. S. Luding, E. Clément, A. Blumen, J. Rajchenbach, and J. Duran. The onset of convection in molecular dynamics simulations of grains. *Phys. Rev. E*, 50:R1762, 1994.
35. S. Luding, E. Clément, A. Blumen, J. Rajchenbach, and J. Duran. Interaction laws and the detachment effect in granular media. In *Fractal Aspects of Materials*, volume 367, page 495, Pittsburgh, Pennsylvania, 1995. Materials Research Society, Symposium Proceedings.